Oblique parameters in gauged baryon and lepton numbers with a 125 GeV Higgs *

YANG Xiu-Yi(杨秀一)[1,2;1)] NIE Jing(聂晶)[3,1]

[1] School of Science, University of Science and Technology Liaoning, Anshan 114051, China
[2] School of Physics, Shandong University, Jinan 250100, China
[3] Department of Physics, Dalian University of Technology, Dalian 116024, China

Abstract: In an extension of the standard model, where baryon number and lepton number are local gauge symmetries, we analyze the effect of corrections from exotic fermions and scalars on the oblique parameters S, T, U. Because a light neutral Higgs h_0 with mass around 124–126 GeV strongly constrains the corresponding parameter space of this model, we also investigate the gluon fusion process $\mathrm{gg}\rightarrow\mathrm{h}_0$ and two photon decay of the lightest neutral Higgs $\mathrm{h}_0\rightarrow\gamma\gamma$ at the Large Hadron Collider.

Key words: local gauge symmetry, baryon and lepton numbers, Higgs

PACS: 14.80.Rt, 11.10Kk, 04.50.-h **DOI:** 10.1088/1674-1137/38/5/053101

1 Introduction

The main physics goals of the Large Hadron Collider (LHC) are to understand the origin of electroweak symmetry breaking, and to search for the neutral Higgs boson predicted by the standard model (SM) and its various extensions. Recently, ATLAS and CMS have reported significant excess events that are interpreted to be most probably related to a neutral Higgs with mass $m_{\mathrm{h}_0}\sim$124–126 GeV. This implies that the Higgs mechanism of breaking electroweak symmetry possibly has a solid experimental cornerstone.

The oblique parameters S, T, U [1] are extracted from electroweak precision data (EWPD) observations that probe the radiative corrections with sufficient accuracy. A light neutral Higgs with mass 124–126 GeV also affects the theoretical evaluations of the oblique parameters S, T, U through loop corrections to the gauge boson propagators, which contain the neutral Higgs as a virtual field. In extensions of the SM, the corrections from the exotic fields to the gauge boson propagators can be expressed in terms of shifts of the parameters S, T, U [2].

A broken baryon number (B) conservation can explain the origin of the matter-antimatter asymmetry in the Universe in a natural way. The heavy majorana neutrinos contained in the seesaw mechanism can induce the tiny observed neutrino masses [3] to explain the results of neutrino oscillation experiments. Hence, the lepton number (L) is also expected to be broken. In Ref. [4], two extensions to the SM are examined, where B and L are spontaneously broken gauge symmetries around the TeV scale, while Ref. [5] also investigates the predictions for the Higgs mass and the Higgs decays in a supersymmetric model named BLMSSM, which is a minimal supersymmetric extension of the SM (MSSM) with local gauged B and L. Within the framework of the first extension of the SM with spontaneously broken B and L [4], we analyze the gluon fusion production and then decay into two photons of the Higgs with mass $m_{\mathrm{h}_0}\sim$124–126 GeV. Additionally, we also investigate the corrections from exotic fields of the oblique parameters S, T, U.

This paper is organized as follows. In Section 2, we briefly summarize the main ingredients of an extension of the SM where the baryon and lepton numbers are local symmetries, we then present the mass squared matrices for the neutral Higgs sector. Inspired by the new results from the ATLAS and CMS collaborations, in Section 3 we study in great detail the Higgs production through gluon fusion, followed by the decay of the Higgs boson into two photons. We discuss the constraints on the parameter space from the oblique parameters S, T, U in Section 4. Our conclusions are given in Section 5.

Received 1 April 2013, Revised 17 December 2013

∗ Supported by National Natural Science Foundation of China (11247019) and Science and Technology Department of Liaoning (2012062)

1) E-mail: yxyruxi@163.com

2 An extension of the SM where baryon and lepton numbers are local gauge symmetries

When baryon and lepton numbers are local gauge symmetries, one can write the gauge group as $SU(3)_{\rm C}\otimes SU(2)_{\rm L}\otimes U(1)_{\rm Y}\otimes U(1)_{\rm B}\otimes U(1)_{\rm L}$. In the first extension of the SM proposed in Ref. [4], the exotic particles include new quarks $Q'_{\rm L}$, $u'_{\rm R}$, $d'_{\rm R}$, new leptons $l'_{\rm L}$, $\nu'_{\rm R}$, $e'_{\rm R}$ and three scalar singlets $S_{\rm B}$, $S_{\rm L}$, S along with a scalar doublet ϕ. The Yukawa couplings are written as

$$\begin{aligned}-\mathcal{L}_{\rm Y} =& \Bigg\{\sum_{I,J=1}^{3}\Big[(Y_{\rm U})_{IJ}\bar{Q}_{\rm L}^I\tilde{H}u_{\rm R}^J+(Y_{\rm D})_{IJ}\bar{Q}_{\rm L}^I H d_{\rm R}^J\Big]\\ &+Y'_{\rm U}\bar{Q}'_{\rm L}Q'^{c}_{\rm L}S_{\rm B}+\sum_{I=1}^{3}\Big[(Y_1)_I\bar{Q}'_{\rm L}\tilde{\phi}u_{\rm R}^J+(Y_2)_I\bar{Q}_{\rm L}^I\phi d'_{\rm R}\Big]\\ &+{\rm h.c.}\Bigg\}+\Bigg\{\sum_{I,J=1}^{3}[(Y_\nu)_{IJ}\bar{L}_{\rm L}^I\tilde{H}\nu_{\rm R}^J+(Y_{\rm E})_{IJ}\bar{L}_{\rm L}^I He_{\rm R}^J]\\ &+Y'_{\rm E}\bar{L}'_{\rm L}L'^{c}_{\rm L}S_{\rm L}+\frac{1}{2}\sum_{I,J=1}^{3}(\lambda_{\rm a})_{IJ}\bar{\nu}_{\rm R}^{I,c}S_{\rm L}^*\nu_{\rm R}^J\\ &+\sum_{I=1}^{3}(\lambda_{\rm b})_I\bar{\nu}_{\rm R}^{I,c}S_{\rm L}\nu'_{\rm R}+{\rm h.c.}\Bigg\}. \qquad (1)\end{aligned}$$

The scalar potential is generally given as follows:

$$\begin{aligned}-\mathcal{L}_{\rm S} =& m_{\rm H}^2H^\dagger H+m_{\phi}^2\phi^\dagger\phi+m_{S_{\rm B}}^2S_{\rm B}^*S_{\rm B}+m_{S_{\rm L}}^2S_{\rm L}^*S_{\rm L}\\ &+m_{\rm S}^2S^*S+\lambda_{\rm HH}(H^\dagger H)(H^\dagger H)+\lambda_{\phi\phi}(\phi^\dagger\phi)(\phi^\dagger\phi)\\ &+\lambda_{\rm BB}(S_{\rm B}^*S_{\rm B})(S_{\rm B}^*S_{\rm B})+\lambda_{\rm LL}(S_{\rm L}^*S_{\rm L})(S_{\rm L}^*S_{\rm L})\\ &+\lambda_{\rm SS}(S^*S)(S^*S)+\lambda_{\rm H\phi}(H^\dagger H)(\phi^\dagger\phi)\\ &+\lambda_{\rm HB}(H^\dagger H)(S_{\rm B}^*S_{\rm B})+\lambda_{\rm HL}(H^\dagger H)(S_{\rm L}^*S_{\rm L})\\ &+\lambda_{\rm HS}(H^\dagger H)(S^*S)+\lambda_{\rm \phi B}(\phi^\dagger\phi)(S_{\rm B}^*S_{\rm B})\\ &+\lambda_{\rm \phi L}(\phi^\dagger\phi)(S_{\rm L}^*S_{\rm L})+\lambda_{\rm \phi S}(\phi^\dagger\phi)(S^*S)\\ &+\lambda_{\rm BL}(S_{\rm B}^*S_{\rm B})(S_{\rm L}^*S_{\rm L})+\lambda_{\rm BS}(S_{\rm B}^*S_{\rm B})(S^*S)\\ &+\lambda_{\rm LS}(S_{\rm L}^*S_{\rm L})(S^*S)+\lambda'_{\rm H\phi}(H^\dagger\phi)(\phi^\dagger H)\\ &+[\mu_1(H^\dagger\phi)S+\mu_2S_{\rm B}^*S^2+{\rm h.c.}]. \qquad (2)\end{aligned}$$

When the $SU(2)_{\rm L}$ doublet H and $SU(2)_{\rm L}$ singlets $S_{\rm B}$, $S_{\rm L}$ acquire the nonzero vacuum expectation values (VEVs) υ, $\upsilon_{\rm B,L}$,

$$\begin{aligned}H =& \begin{pmatrix} G^+ \\ \frac{1}{\sqrt{2}}(\upsilon+H_0+{\rm i}G^0)\end{pmatrix},\\ S_{\rm B} =& \frac{1}{\sqrt{2}}(\upsilon_{\rm B}+S_{\rm B}^0+{\rm i}G_{\rm B}^0),\\ S_{\rm L} =& \frac{1}{\sqrt{2}}(\upsilon_{\rm L}+S_{\rm L}^0+{\rm i}G_{\rm L}^0), \qquad (3)\end{aligned}$$

the local gauge symmetry $SU(2)_{\rm L}\otimes U(1)_{\rm Y}\otimes U(1)_{\rm B}\otimes U(1)_{\rm L}$ is broken down to the electromagnetic symmetry $U(1)_{\rm e}$, where G^+, G^0, $G_{\rm B}^0$ and $G_{\rm L}^0$ denote massless Goldstone bosons. Correspondingly, the mass terms for the neutral Higgs are formulated as

$$-\mathcal{L}_{\rm mass}^{\rm H}=\frac{1}{2}\Big(H_0,\ S_{\rm B}^0,\ S_{\rm L}^0\Big)m_{\rm CPE}^2\begin{pmatrix}H_0\\ S_{\rm B}^0\\ S_{\rm L}^0\end{pmatrix}, \qquad (4)$$

where the symmetric 3×3 mass squared matrix $m_{\rm CPE}^2$ is

$$m_{\rm CPE}^2=\begin{pmatrix}2\lambda_{\rm HH}\upsilon^2 & \lambda_{\rm HB}\upsilon\upsilon_{\rm B} & \lambda_{\rm HL}\upsilon\upsilon_{\rm L}\\ \lambda_{\rm HB}\upsilon\upsilon_{\rm B} & 2\lambda_{\rm BB}\upsilon_{\rm B}^2 & \lambda_{\rm BL}\upsilon_{\rm B}\upsilon_{\rm L}\\ \lambda_{\rm HL}\upsilon\upsilon_{\rm L} & \lambda_{\rm BL}\upsilon_{\rm B}\upsilon_{\rm L} & 2\lambda_{\rm LL}\upsilon_{\rm L}^2\end{pmatrix}. \qquad (5)$$

Through the orthogonal 3×3 transformation matrix $Z_{\rm CPE}$, the mass squared matrix $m_{\rm CPE}^2$ can be diagonalized as

$$Z_{\rm CPE}^{\rm T}m_{\rm CPE}^2Z_{\rm CPE}=\Big(m_{\rm H_1^0}^2,\ m_{\rm H_2^0}^2,\ m_{\rm H_3^0}^2\Big), \qquad (6)$$

where $m_{\rm H_1^0}=m_{\rm h_0}\approx125$ GeV.

In a similar way, we can write the $SU(2)_{\rm L}$ doublet ϕ and the $SU(2)_{\rm L}$ singlet S as

$$\begin{aligned}\phi=&\begin{pmatrix}\phi^+\\ \frac{1}{\sqrt{2}}\Big(\phi_{\rm R}^0+{\rm i}\phi_{\rm I}^0\Big)\end{pmatrix},\\ S=&\frac{1}{\sqrt{2}}\Big(S_{\rm R}^0+{\rm i}S_{\rm I}^0\Big). \qquad (7)\end{aligned}$$

Since the local gauge symmetry $SU(2)_{\rm L}\otimes U(1)_{\rm Y}\otimes U(1)_{\rm B}\otimes U(1)_{\rm L}$ is broken down to the electromagnetic symmetry $U(1)_{\rm e}$, the terms in square brackets in Eq. (2) induce mixing among the neutral scalar particles $\phi_{\rm R}^0$, $\phi_{\rm I}^0$, $S_{\rm R}^0$, $S_{\rm I}^0$, and the mass terms are written as

$$-\mathcal{L}_{mass}^{\Phi}=\frac{1}{2}\Big(\phi_{\rm R}^0,\ S_{\rm R}^0,\ \phi_{\rm I}^0,\ S_{\rm I}^0\Big)m_{\rm CPM}^2\begin{pmatrix}\phi_{\rm R}^0\\ S_{\rm R}^0\\ \phi_{\rm I}^0\\ S_{\rm I}^0\end{pmatrix}, \qquad (8)$$

with the symmetric 4×4 mass squared matrix $m_{\rm CPM}^2$ being

$$m^2_{\rm CPM}=\begin{pmatrix} m^2_\phi & \sqrt{2}\upsilon\Re(\mu_1) & 0 & -\sqrt{2}\upsilon\Im(\mu_1) \\ \sqrt{2}\upsilon\Re(\mu_1) & m^2_{\rm S}+2\sqrt{2}\upsilon_{\rm B}\Re(\mu_2) & 0 & -2\sqrt{2}\upsilon_{\rm B}\Im(\mu_2) \\ 0 & 0 & m^2_\phi & -\sqrt{2}\upsilon\Re(\mu_1) \\ -\sqrt{2}\upsilon\Im(\mu_1) & -2\sqrt{2}\upsilon_{\rm B}\Im(\mu_2) & -\sqrt{2}\upsilon\Re(\mu_1) & m^2_{\rm S}+2\sqrt{2}\upsilon_{\rm B}\Re(\mu_2) \end{pmatrix}. \tag{9}$$

We also diagonalize the mass squared matrix $m^2_{\rm CPM}$ through the 4×4 orthogonal rotation $Z_{\rm CPM}$:

$$Z^{\rm T}_{\rm CPM}m^2_{\rm CPM}Z_{\rm CPM}=\left(m^2_{\Phi^0_1},\ m^2_{\Phi^0_2},m^2_{\Phi^0_3},m^2_{\Phi^0_4}\right). \tag{10}$$

Similarly, the mass for the charged scalar $\phi^\pm$ is expressed by

$$m^2_{\phi^\pm}=\frac{1}{2}m^2_\phi-\frac{1}{2}\lambda'_{\rm H\phi}\upsilon^2. \tag{11}$$

Since the field ϕ does not get a nonzero VEV after the electroweak symmetry is broken down, there is no mass mixing between the exotic quarks and the SM quarks.

In the left-handed basis $(\nu^I_{\rm L},\ \nu'_{\rm L},\ \nu'^c_{\rm R},\ \nu^{I,c}_{\rm R})$, $(I=1,\ 2,\ 3)$, the mass matrix for neutrinos is given by the 8×8 matrix

$$\mathcal{M}_{\rm n}=\begin{pmatrix} 0_{3\times3} & \left(M_{\rm D}\right)_{3\times5} \\ \left(M^{\rm T}_{\rm D}\right)_{5\times3} & \left(M_{\rm N}\right)_{5\times5}\end{pmatrix}. \tag{12}$$

Here, the 3×5 matrix $M_{\rm D}$ is written as

$$M_{\rm D}=\left(0_{3\times2},\ \frac{\upsilon}{\sqrt{2}}\left(Y^*_\nu\right)_{3\times3}\right), \tag{13}$$

and the 5×5 matrix $M_{\rm N}$ is

$$M_{\rm N}=\begin{pmatrix} 0, & \frac{\upsilon}{\sqrt{2}}Y'^*_\nu, & 0_{1\times3} \\ \frac{\upsilon}{\sqrt{2}}Y'^*_\nu, & 0, & \frac{\upsilon_{\rm L}}{\sqrt{2}}(\lambda^*_{\rm b})_{1\times3} \\ 0_{3\times1}, & \frac{\upsilon_{\rm L}}{\sqrt{2}}(\lambda^\dagger_{\rm b})_{3\times1}, & \frac{\upsilon_{\rm L}}{\sqrt{2}}(\lambda^\dagger_{\rm a})_{3\times3}\end{pmatrix}, \tag{14}$$

By integrating the heavy freedoms out, we get the following mass matrix for three light neutrinos:

$$\mathcal{M}_\nu=-M_{\rm D}M^{-1}_{\rm N}M^{\rm T}_{\rm D}, \tag{15}$$

which is diagonalized by the Pontecorvo-Maki-Nakagawa-Sakata matrix $U_{\rm PMNS}$

$$U^{\rm T}_{\rm PMNS}\mathcal{M}_\nu U_{\rm PMNS}={\rm diag}(m_{\nu_1},m_{\nu_2},m_{\nu_3}). \tag{16}$$

Meanwhile, the Majorana mass matrix $M_{\rm N}$ is similarly diagonalized by a 5×5 matrix $Z_{\rm N}$

$$Z^{\rm T}_{\rm N}M_{\rm N}Z_{\rm N}={\rm diag}(m_{\rm N_1},m_{\rm N_2},m_{\rm N_3},m_{\rm N_4},m_{\rm N_5}). \tag{17}$$

3 The $\mathrm{gg}\to \mathrm{h_0}\to\gamma\gamma$ process in gauged baryon and lepton numbers

At the LHC, the Higgs is produced chiefly through gluon fusion. In the SM, the leading order (LO) contributions originate from the one-loop diagram, which involves virtual top quarks. The cross section for this process is known as the next-to-next-to-leading order (NNLO) [6], which can enhance the LO result by 80%–100%. Furthermore, any new particle that couples strongly with the Higgs can significantly modify this cross section. In the extension of the SM considered here, the LO decay width for the process $\rm h_0\to gg$ is given by (see Ref. [7] and the references therein)

$$\Gamma_{\rm NP}({\rm h_0\to gg})=\frac{G_{\rm F}\alpha^2_s m^3_{\rm h_0}|(Z_{\rm CPE})_{11}|^2}{64\sqrt{2}\pi^3}\Big|A_{1/2}(x_{\rm t})+A_{1/2}(x_{\rm t'})+A_{1/2}(x_{\rm b'})\Big|^2, \tag{18}$$

where $x_{\rm a}=m^2_{\rm h_0}/(4m^2_{\rm a})$, a=t, t′, b′, and the loop function $A_{1/2}$ is defined as given in the Appendix.

The Higgs to diphoton decay is also obtained from loop diagrams. The LO contributions are derived from the one-loop diagrams containing virtual charged gauge bosons $\rm W^\pm$ or virtual top quarks in the SM. In this model, the additional charged scalar $\phi^\pm$ and exotic fermions t′, b′, τ′ contribute corrections to the decay width of the Higgs to diphoton at LO. The corresponding expression is written as

$$\begin{aligned}\Gamma_{\rm NP}({\rm h_0}\to\gamma\gamma)=\frac{G_{\rm F}\alpha^2 m^3_{\rm h_0}}{128\sqrt{2}\pi^3}\Big|&(Z_{\rm CPE})_{11}\Big(\frac{4}{3}A_{1/2}(x_{\rm t})+\frac{4}{3}A_{1/2}(x_{\rm t'})+\frac{1}{3}A_{1/2}(x_{\rm b'})+A_{1/2}(x_{\tau'})+A_1(x_{\rm W})\Big)\\ &+\frac{8m^2_{\rm W}s^2_{\rm W}}{{\rm e}^2m^2_{\phi^\pm}}\Big(\lambda_{\rm H\phi}(Z_{\rm CPE})_{11}+\frac{\upsilon_{\rm B}}{\upsilon}\lambda_{\rm \phi B}(Z_{\rm CPE})_{21}+\frac{\upsilon_{\rm L}}{\upsilon}\lambda_{\rm \phi L}(Z_{\rm CPE})_{31}\Big)A_0(x_{\phi^\pm})\Big|^2,\end{aligned} \tag{19}$$

the concrete expressions for the loop functions A_0, A_1

are given in the Appendix.

The Higgs discoveries from both the ATLAS and CMS experiments have observed an excess in Higgs production and decay into the diphoton channel, which is a factor of 1.4–2 times larger than the SM expectations. The observed signal for the diphoton channels is quantified by the ratio

$$R_{\gamma\gamma}=\frac{\Gamma_{\rm NP}(\mathrm{h}_0\to\mathrm{gg})\Gamma_{\rm NP}(\mathrm{h}_0\to\gamma\gamma)}{\Gamma_{\rm SM}(\mathrm{h}_0\to\mathrm{gg})\Gamma_{\rm SM}(\mathrm{h}_0\to\gamma\gamma)}, \tag{20}$$

where we assume that all exotic fields are heavier than the lightest Higgs h_0. The current value of this ratio is as follows [8, 9]:

$$\begin{aligned}&\text{ATLAS}: R_{\gamma\gamma}=1.90\pm0.5,\\ &\text{CMS}: R_{\gamma\gamma}=1.56\pm0.43,\\ &\text{ATLAS+CMS}: R_{\gamma\gamma}=1.71\pm0.33.\end{aligned} \tag{21}$$

Note that the combination of the ATLAS and CMS results is taken from Ref. [10].

4 Corrections to the oblique parameters

A common approach to constrain physics beyond the SM is to use global electroweak fitting through the oblique parameters S, T, U [1]. In the SM, electroweak precision tests imply a relationship between m_{h_0} and $m_{\rm Z}$. In the model considered here, the electroweak precision tests also strongly constrain the mass spectrum and relevant couplings.

Here, we adopt the definitions of the oblique parameters S, T, U given in [1, 11]:

$$\begin{aligned}S &= 16\pi\left\{\frac{\Pi_{33}(m_{\rm Z}^2)-\Pi_{33}(0)}{m_{\rm Z}^2}-\frac{\Pi_{3\rm Q}(m_{\rm Z}^2)-\Pi_{3\rm Q}(0)}{m_{\rm Z}^2}\right\},\\ T &= 4\pi\frac{\Pi_{11}(0)-\Pi_{33}(0)}{m_{\rm Z}^2 s_{\rm W}^2 c_{\rm W}^2},\\ U &= 16\pi\left\{\frac{\Pi_{11}(m_{\rm Z}^2)-\Pi_{11}(0)}{m_{\rm Z}^2}-\frac{\Pi_{33}(m_{\rm Z}^2)-\Pi_{33}(0)}{m_{\rm Z}^2}\right\},\end{aligned} \tag{22}$$

where $s_{\rm W}=\sin\theta_{\rm W}$ and $c_{\rm W}=\cos\theta_{\rm W}$ with the Weinberg angle $\theta_{\rm W}$ defined at the energy scale $\mu=m_{\rm Z}$. In the above definitions, Π_{11} and Π_{33} are the vacuum polarizations of isospin currents, and $\Pi_{3\rm Q}$ is the vacuum polarization of one isospin and one hypercharge current.

By comparing the measurable electroweak observables with the theoretical predictions, one finds the fitted values [12]

$$\begin{aligned}\Delta S &= S-S_{\rm SM}=0.04\pm0.10,\\ \Delta T &= T-T_{\rm SM}=0.05\pm0.11,\\ \Delta U &= U-U_{\rm SM}=0.08\pm0.11.\end{aligned} \tag{23}$$

As mentioned above, there is no mass mixing between the exotic quarks and the SM quarks. The corresponding corrections to the oblique parameters from exotic quarks are

$$\begin{aligned}\Delta S_{\rm Q'} &= \frac{1}{\pi}\left\{\int_0^1 \mathrm{d}x x(1-x)\ln\frac{m_{\rm b'}^2-x(1-x)m_{\rm Z}^2}{m_{\rm t'}^2-x(1-x)m_{\rm Z}^2}-\frac{3m_{\rm t'}^2}{2m_{\rm Z}^2}\int_0^1\mathrm{d}x\ln\frac{m_{\rm t'}^2-x(1-x)m_{\rm Z}^2}{m_{\rm t'}^2}-\frac{3m_{\rm b'}^2}{2m_{\rm Z}^2}\int_0^1\mathrm{d}x\ln\frac{m_{\rm b'}^2-x(1-x)m_{\rm Z}^2}{m_{\rm b'}^2}\right\},\\ \Delta T_{\rm Q'} &= -\frac{3}{4\pi s_{\rm W}^2c_{\rm W}^2}\left\{\frac{m_{\rm t'}^2}{m_{\rm Z}^2}\int_0^1\mathrm{d}x x\ln\frac{xm_{\rm t'}^2+(1-x)m_{\rm b'}^2}{m_{\rm t'}^2}+\frac{m_{\rm b'}^2}{m_{\rm Z}^2}\int_0^1\mathrm{d}x(1-x)\ln\frac{xm_{\rm t'}^2+(1-x)m_{\rm b'}^2}{m_{\rm b'}^2}\right\},\\ \Delta U_{\rm Q'} &= \frac{1}{\pi}\left\{3\int_0^1\mathrm{d}x x(1-x)\ln\frac{[xm_{\rm t'}^2+(1-x)m_{\rm b'}^2-x(1-x)m_{\rm Z}^2]^2}{[m_{\rm t'}^2-x(1-x)m_{\rm Z}^2][m_{\rm b'}^2-x(1-x)m_{\rm Z}^2]}\right.\\ &\quad -3\int_0^1\mathrm{d}x\left(x\frac{m_{\rm t'}^2}{m_{\rm Z}^2}+(1-x)\frac{m_{\rm b'}^2}{m_{\rm Z}^2}\right)\ln\frac{xm_{\rm t'}^2+(1-x)m_{\rm b'}^2-x(1-x)m_{\rm Z}^2}{xm_{\rm t'}^2+(1-x)m_{\rm b'}^2}\\ &\quad \left.-\frac{3m_{\rm t'}^2}{2m_{\rm Z}^2}\int_0^1\mathrm{d}x\ln\frac{m_{\rm t'}^2-x(1-x)m_{\rm Z}^2}{m_{\rm t'}^2}-\frac{3m_{\rm b'}^2}{2m_{\rm Z}^2}\int_0^1\mathrm{d}x\ln\frac{m_{\rm b'}^2-x(1-x)m_{\rm Z}^2}{m_{\rm b'}^2}\right\}.\end{aligned} \tag{24}$$

Here, $m_{\rm b'}$ and $m_{\rm t'}$ denote the masses of the charged $-1/3$ exotic quark b' and the charged $2/3$ exotic quark t', respectively.

In a similar way, there is no mass mixing between the exotic charged leptons and the SM leptons. Ignoring the tiny mixing between the left-handed neutrinos and heavy majorana neutrinos, we write the corrections to the oblique parameters from exotic leptons as

$$\Delta S_{\mathrm{L}'} = \frac{1}{\pi}\sum_{i,j=1}^{5}(Z_{\mathrm{N}})_{1i}(Z_{\mathrm{N}}^{\dagger})_{i1}(Z_{\mathrm{N}})_{1j}(Z_{\mathrm{N}}^{\dagger})_{j1}\Bigg\{-\frac{1}{2}\int_0^1\mathrm{d}x\left(x\frac{m_{\mathrm{N_i}}^2}{m_{\mathrm{Z}}^2}+(1-x)\frac{m_{\mathrm{N}_j}^2}{m_{\mathrm{Z}}^2}\right)$$
$$\times\ln\frac{xm_{\mathrm{N}_i}^2+(1-x)m_{\mathrm{N}_j}^2-x(1-x)m_{\mathrm{Z}}^2}{xm_{\mathrm{N}_i}^2+(1-x)m_{\mathrm{N}_j}^2}-\frac{m_{\tau'}^2}{2m_{\mathrm{Z}}^2}\int_0^1\mathrm{d}x\ln\frac{m_{\tau'}^2-x(1-x)m_{\mathrm{Z}}^2}{m_{\tau'}^2}$$
$$+\int_0^1\mathrm{d}xx(1-x)\ln\frac{xm_{\mathrm{N}_i}^2+(1-x)m_{\mathrm{N}_j}^2-x(1-x)m_{\mathrm{Z}}^2}{m_{\tau'}^2-x(1-x)m_{\mathrm{Z}}^2}\Bigg\},$$

$$\Delta T_{\mathrm{L}'} = -\frac{1}{4\pi s_{\mathrm{W}}^2c_{\mathrm{W}}^2}\sum_{i,j=1}^{5}(Z_{\mathrm{N}})_{1i}(Z_{\mathrm{N}}^{\dagger})_{i1}(Z_{\mathrm{N}})_{1j}(Z_{\mathrm{N}}^{\dagger})_{j1}\Bigg\{\frac{m_{\mathrm{N}_i}^2}{m_{\mathrm{Z}}^2}\int_0^1\mathrm{d}x\ln\frac{xm_{\mathrm{N}_i}^2+(1-x)m_{\tau'}^2}{xm_{\mathrm{N}_i}^2+(1-x)m_{\mathrm{N}_j}^2}$$
$$+\frac{m_{\tau'}^2}{m_{\mathrm{Z}}^2}\int_0^1\mathrm{d}x(1-x)\ln\frac{xm_{\mathrm{N}_i}^2+(1-x)m_{\tau'}^2}{m_{\tau'}^2}\Bigg\},$$

$$\Delta U_{\mathrm{L}'} = \frac{1}{\pi}\sum_{i,j=1}^{5}(Z_{\mathrm{N}})_{1i}(Z_{\mathrm{N}}^{\dagger})_{i1}(Z_{\mathrm{N}})_{1j}(Z_{\mathrm{N}}^{\dagger})_{j1}\Bigg\{\frac{m_{\tau'}^2}{2m_{\mathrm{Z}}^2}\int_0^1\mathrm{d}x\ln\frac{m_{\tau'}^2-x(1-x)m_{\mathrm{Z}}^2}{m_{\tau'}^2}$$
$$+\int_0^1\mathrm{d}xx(1-x)\ln\frac{[xm_{\mathrm{N}_i}^2+(1-x)m_{\tau'}^2-x(1-x)m_{\mathrm{Z}}^2]^2}{(xm_{\mathrm{N}_i}^2+(1-x)m_{\mathrm{N}_j}^2-x(1-x)m_{\mathrm{Z}}^2)(m_{\tau'}^2-x(1-x)m_{\mathrm{Z}}^2)}$$
$$-\int_0^1\mathrm{d}x\left(x\frac{m_{\mathrm{N}_i}^2}{m_{\mathrm{Z}}^2}+(1-x)\frac{m_{\tau'}^2}{m_{\mathrm{Z}}^2}\right)\ln\frac{xm_{\mathrm{N}_i}^2+(1-x)m_{\tau'}^2-x(1-x)m_{\mathrm{Z}}^2}{xm_{\mathrm{N}_i}^2+(1-x)m_{\tau'}^2}$$
$$+\frac{1}{2}\int_0^1\mathrm{d}x\left(x\frac{m_{\mathrm{N}_i}^2}{m_{\mathrm{Z}}^2}+(1-x)\frac{m_{\mathrm{N}_j}^2}{m_{\mathrm{Z}}^2}\right)\ln\frac{xm_{\mathrm{N}_i}^2+(1-x)m_{\mathrm{N}_j}^2-x(1-x)m_{\mathrm{Z}}^2}{xm_{\mathrm{N}_i}^2+(1-x)m_{\mathrm{N}_j}^2}\Bigg\}. \tag{25}$$

Here, the 5×5 unitary matrix Z_{N} is the mixing matrix for heavy majorana neutrinos, m_{N_i} $(i=1,\ 2,\ \cdots,5)$ are the corresponding masses of the heavy neutrinos, and $m_{\tau'}$ is the mass of the charged exotic lepton τ'.

Since the radiative corrections to the self energy of gauge bosons originate from three CP-even Higgs (h_0, H_2^0, H_3^0), the corresponding contributions to the oblique parameters are given by

$$\Delta S_{\mathrm{H}} = \frac{1}{\pi}\sum_{i=1}^{3}(Z_{\mathrm{CPE}})_{1i}^2\Bigg\{\frac{1}{2}\int_0^1\mathrm{d}xx(1-x)\ln\frac{x^2m_{\mathrm{Z}}^2+(1-x)m_{\mathrm{H}_i^0}^2}{m_{\mathrm{Z}}^2}+\int_0^1\mathrm{d}x\left(1-\frac{x}{2}-(1-x)\frac{m_{\mathrm{H}_i^0}^2}{2m_{\mathrm{Z}}^2}\right)\ln\frac{x^2m_{\mathrm{Z}}^2+(1-x)m_{\mathrm{H}_i^0}^2}{xm_{\mathrm{Z}}^2+(1-x)m_{\mathrm{H}_i^0}^2}\Bigg\},$$

$$\Delta T_{\mathrm{H}} = \frac{1}{4\pi s_{\mathrm{W}}^2c_{\mathrm{W}}^2}\sum_{i=1}^{3}(Z_{\mathrm{CPE}})_{1i}^2\Bigg\{-\int_0^1\mathrm{d}x\left(1-\frac{x}{2}-(1-x)\frac{m_{\mathrm{H}_i^0}^2}{2m_{\mathrm{Z}}^2}\right)\ln\frac{xm_{\mathrm{Z}}^2+(1-x)m_{\mathrm{H}_i^0}^2}{m_{\mathrm{Z}}^2}$$
$$+\int_0^1\mathrm{d}x\left(\left(1-\frac{x}{2}\right)c_{\mathrm{W}}^2-(1-x)\frac{m_{\mathrm{H}_i^0}^2}{2m_{\mathrm{Z}}^2}\right)\ln\frac{xm_{\mathrm{W}}^2+(1-x)m_{\mathrm{H}_i^0}^2}{m_{\mathrm{Z}}^2}\Bigg\},$$

$$\Delta U_{\mathrm{H}} = \frac{1}{\pi}\sum_{i=1}^{3}(Z_{\mathrm{CPE}})_{1i}^2\Bigg\{\frac{1}{2}\int_0^1\mathrm{d}x\left(x^2+(1-x)\frac{m_{\mathrm{H}_i^0}^2}{m_{\mathrm{Z}}^2}\right)\ln\frac{x^2m_{\mathrm{Z}}^2+(1-x)m_{\mathrm{H}_i^0}^2}{m_{\mathrm{Z}}^2}-\int_0^1\mathrm{d}x\ln\frac{x^2m_{\mathrm{Z}}^2+(1-x)m_{\mathrm{H}_i^0}^2}{xm_{\mathrm{Z}}^2+(1-x)m_{\mathrm{H}_i^0}^2}$$
$$-\frac{1}{2}\int_0^1\mathrm{d}x\left(x+(1-x)\frac{m_{\mathrm{H}_i^0}^2}{m_{\mathrm{Z}}^2}\right)\ln\frac{xm_{\mathrm{Z}}^2+(1-x)m_{\mathrm{H}_i^0}^2}{m_{\mathrm{Z}}^2}+\int_0^1\mathrm{d}x\left(\left(1-\frac{x}{2}\right)c_{\mathrm{W}}^2-(1-x)\frac{m_{\mathrm{H}_i^0}^2}{2m_{\mathrm{Z}}^2}\right)\ln\frac{xm_{\mathrm{W}}^2+(1-x)m_{\mathrm{H}_i^0}^2-x(1-x)m_{\mathrm{Z}}^2}{xm_{\mathrm{W}}^2+(1-x)m_{\mathrm{H}_i^0}^2}$$

$$+\frac{1}{2}\int_0^1 \mathrm{d}x x(1-x)\ln\frac{xm_{\mathrm{W}}^2+(1-x)m_{\mathrm{H}_i^0}^2-x(1-x)m_{\mathrm{Z}}^2}{m_{\mathrm{Z}}^2}\Bigg\}. \tag{26}$$

Here, we adopt the notation H_1^0 to represent the lightest neutral Higgs h_0. In addition, the contributions from Φ_i^0 and $\phi^{\pm}$ to the oblique parameters are formulated as follows

$$\begin{aligned}
\Delta S_\phi = & \frac{1}{2\pi}\Bigg\{\sum_{i,j}^{4}(Z_{\mathrm{CPM}})_{1i}^2(Z_{\mathrm{CPM}})_{3j}^2\Bigg[-\int_0^1\mathrm{d}x\left(x\frac{m_{\Phi_i^0}^2}{m_{\mathrm{Z}}^2}+(1-x)\frac{m_{\Phi_j^0}^2}{m_{\mathrm{Z}}^2}\right)\ln\frac{xm_{\Phi_i^0}^2+(1-x)m_{\Phi_j^0}^2-x(1-x)m_{\mathrm{Z}}^2}{xm_{\Phi_i^0}^2+(1-x)m_{\Phi_j^0}^2} \\
& -\int_0^1\mathrm{d}x x(1-x)\ln\frac{xm_{\Phi_i^0}^2+(1-x)m_{\Phi_j^0}^2-x(1-x)m_{\mathrm{Z}}^2}{m_{\phi^\pm}^2-x(1-x)m_{\mathrm{Z}}^2}\Bigg]+\frac{m_{\phi^\pm}^2}{m_{\mathrm{Z}}^2}\int_0^1\mathrm{d}x\ln\frac{m_{\phi^\pm}^2-x(1-x)m_{\mathrm{Z}}^2}{m_{\phi^\pm}^2}\Bigg\}, \\
\Delta T_\phi = & \frac{1}{8\pi s_{\mathrm{W}}^2c_{\mathrm{W}}^2}\Bigg\{-\sum_{i=1}^{4}\Big[(Z_{\mathrm{CPM}})_{1i}^2+(Z_{\mathrm{CPM}})_{3i}^2\Big]\Bigg[\frac{m_{\phi^\pm}^2}{m_{\mathrm{Z}}^2}\int_0^1\mathrm{d}x x\ln\frac{xm_{\phi^\pm}^2+(1-x)m_{\Phi_i^0}^2}{m_{\phi^\pm}^2}+\frac{m_{\Phi_i^0}^2}{m_{\mathrm{Z}}^2}\int_0^1\mathrm{d}x x\ln\frac{xm_{\Phi_i^0}^2+(1-x)m_{\phi^\pm}^2}{m_{\Phi_i^0}^2}\Bigg] \\
& +\sum_{i,j}^{4}(Z_{\mathrm{CPM}})_{1i}^2(Z_{\mathrm{CPM}})_{3j}^2\int_0^1\mathrm{d}x\left(x\frac{m_{\Phi_i^0}^2}{m_{\mathrm{Z}}^2}+(1-x)\frac{m_{\Phi_j^0}^2}{m_{\mathrm{Z}}^2}\right)\ln\frac{xm_{\Phi_i^0}^2+(1-x)m_{\Phi_j^0}^2}{m_{\Phi_i^0}^2}\Bigg\}, \\
\Delta U_\phi = & \frac{1}{2\pi}\Bigg\{-\sum_{i=1}^{4}\Big[(Z_{\mathrm{CPM}})_{1i}^2+(Z_{\mathrm{CPM}})_{3i}^2\Big]\Bigg[\int_0^1\mathrm{d}x\left(x\frac{m_{\phi^\pm}^2}{m_{\mathrm{Z}}^2}+(1-x)\frac{m_{\Phi_i^0}^2}{m_{\mathrm{Z}}^2}\right)\ln\frac{xm_{\phi^\pm}^2+(1-x)m_{\Phi_i^0}^2-x(1-x)m_{\mathrm{Z}}^2}{xm_{\phi^\pm}^2+(1-x)m_{\Phi_i^0}^2} \\
& +\frac{1}{2}\int_0^1\mathrm{d}x x(1-x)\ln\frac{xm_{\phi^\pm}^2+(1-x)m_{\Phi_i^0}^2-x(1-x)m_{\mathrm{Z}}^2}{m_{\phi^\pm}^2-x(1-x)m_{\mathrm{Z}}^2}\Bigg]+\sum_{i,j}^{4}(Z_{\mathrm{CPM}})_{1i}^2(Z_{\mathrm{CPM}})_{3j}^2\Bigg[\int_0^1\mathrm{d}x\left(x\frac{m_{\Phi_i^0}^2}{m_{\mathrm{Z}}^2}+(1-x)\frac{m_{\Phi_j^0}^2}{m_{\mathrm{Z}}^2}\right) \\
& \times\ln\frac{xm_{\Phi_i^0}^2+(1-x)m_{\Phi_j^0}^2-x(1-x)m_{\mathrm{Z}}^2}{xm_{\Phi_i^0}^2+(1-x)m_{\Phi_j^0}^2}+\int_0^1\mathrm{d}x x(1-x)\ln\frac{xm_{\Phi_i^0}^2+(1-x)m_{\Phi_j^0}^2-x(1-x)m_{\mathrm{Z}}^2}{xm_{\Phi_i^0}^2+(1-x)m_{\phi^\pm}^2-x(1-x)m_{\mathrm{Z}}^2} \\
& +\int_0^1\mathrm{d}x x(1-x)\ln\frac{xm_{\Phi_i^0}^2+(1-x)m_{\Phi_j^0}^2-x(1-x)m_{\mathrm{Z}}^2}{xm_{\phi^\pm}^2+(1-x)m_{\Phi_j^0}^2-x(1-x)m_{\mathrm{Z}}^2}\Bigg]+\frac{m_{\phi^\pm}^2}{m_{\mathrm{Z}}^2}\int_0^1\mathrm{d}x\ln\frac{m_{\phi^\pm}^2-x(1-x)m_{\mathrm{Z}}^2}{m_{\phi^\pm}^2}\Bigg\}. \qquad (27)
\end{aligned}$$

5 Numerical analysis

As mentioned above, the most stringent constraint on the parameter space is that the 3×3 mass squared matrix in Eq. (5) should produce the lightest eigenvector with a mass m_{h_0}=125 GeV.

In order to make the final results consistent with this condition, we require the self coupling of the Higgs doublet to satisfy

$$\lambda_{\mathrm{HH}}=\frac{A}{B}, \tag{28}$$

where

$$\begin{aligned}
A = & m_{\mathrm{h}_0}^6-2\Big[\lambda_{\mathrm{BB}}\upsilon_{\mathrm{B}}^2+\lambda_{\mathrm{LL}}\upsilon_{\mathrm{L}}^2\Big]m_{\mathrm{h}_0}^4+\Big[(4\lambda_{\mathrm{BB}}\lambda_{\mathrm{LL}}-\lambda_{\mathrm{BL}}^2)\upsilon_{\mathrm{B}}^2\upsilon_{\mathrm{L}}^2 \\
& -\lambda_{\mathrm{HB}}^2\upsilon^2\upsilon_{\mathrm{B}}^2-\lambda_{\mathrm{HL}}^2\upsilon^2\upsilon_{\mathrm{L}}^2\Big]m_{\mathrm{h}_0}^2+2\Big[\lambda_{\mathrm{BB}}\lambda_{\mathrm{HL}}^2+\lambda_{\mathrm{LL}}\lambda_{\mathrm{HB}}^2 \\
& -\lambda_{\mathrm{HB}}\lambda_{\mathrm{HL}}\lambda_{\mathrm{BL}}\Big]\upsilon^2\upsilon_{\mathrm{B}}^2\upsilon_{\mathrm{L}}^2, \\
B = & 2\upsilon^2\Big[m_{\mathrm{h}_0}^4-2(\lambda_{\mathrm{BB}}\upsilon_{\mathrm{B}}^2+\lambda_{\mathrm{LL}}\upsilon_{\mathrm{L}}^2)m_{\mathrm{h}_0}^2 \\
& +(4\lambda_{\mathrm{BB}}\lambda_{\mathrm{LL}}-\lambda_{\mathrm{BL}}^2)\upsilon_{\mathrm{B}}^2\upsilon_{\mathrm{L}}^2\Big]. \qquad (29)
\end{aligned}$$

The present experimental lower bounds on the fourth generation charged lepton τ', up-type and down-type quarks t' and b' at 95% C.L. are $m_{\tau'}$ >100.8 GeV, $m_{\mathrm{t}'}$ >420 GeV and $m_{\mathrm{b}'}$ >372 GeV, respectively. The fourth generation quarks t' and b' acquire nonzero masses $m_{\mathrm{t}'}=m_{\mathrm{b}'}=\frac{Y_{\mathrm{Q}}'}{\sqrt{2}}\upsilon_{\mathrm{B}}$ when local $U(1)_{\mathrm{B}}$ symmetry is broken. In addition, the charged leptons of the fourth generation τ' obtain nonzero masses $m_{\tau'}=\frac{Y_{\mathrm{E}}'}{\sqrt{2}}\upsilon_{\mathrm{L}}$ when local $U(1)_{\mathrm{L}}$ symmetry is broken.

However, there are too many free parameters in the model considered here. In our numerical analysis, we adopt the assumption on the parameter space

$$\begin{aligned}
m_{\mathrm{t}'} = & m_{\mathrm{b}'}=m_{\tau'}=m_{\mathrm{F}}, \\
\lambda_{\mathrm{BB}} = & \lambda_{\mathrm{LL}}=0.5,\ \lambda_{\mathrm{HL}}=\lambda_{\mathrm{BL}}=\lambda_{\mathrm{HB}}=\lambda_{\mathrm{NP}}, \qquad (30) \\
\lambda_{\phi\mathrm{H}} = & \lambda_{\phi\mathrm{B}}=\lambda_{\phi\mathrm{L}}=\lambda_{\mathrm{NP}}',
\end{aligned}$$

to decrease the number of free parameters in the concerned model. Furthermore, we assume $\upsilon\ll\upsilon_{\mathrm{B,L}}$,

$(\lambda_a)_{3\times 3}$=diag(λ_a, λ_a, λ_a), and choose the hierarchical assumption on Yukawa couplings $\left|(Y_\nu)_{IJ}\right| \ll |Y'_\nu| \sim \lambda_a \sim \lambda_{b_I}$, ($I$, J=1, 2, 3) to obtain our final results. Applying the assumptions above, we obtain the majorana mass for the lightest exotic neutrino N_1 to be

$$m_{N_1} \approx \frac{\upsilon^2}{\sqrt{2}\upsilon_L}\frac{\lambda_a|Y'_\nu|}{\lambda_b^2}, \tag{31}$$

with $\lambda_b^2 = \lambda_{b_1}^2 + \lambda_{b_2}^2 + \lambda_{b_3}^2$. Of course, we need this mass to be greater than $m_Z/2$ in order to be consistent with the measured Z-boson decay width. The masses of other heavy majorana neutrinos are

$$m_{N_i} \approx \left(\frac{\upsilon_L}{\sqrt{2}}\lambda_a, \frac{\upsilon_L}{\sqrt{2}}\lambda_a, \frac{\upsilon_L}{2\sqrt{2}}(\Delta-\lambda_a), \frac{\upsilon_L}{2\sqrt{2}}(\Delta+\lambda_a)\right), \tag{32}$$

for i=2, 3, 4, 5 and $\Delta = \sqrt{\lambda_a^2 + 4\lambda_b^2}$.

Correspondingly, the 5×5 mixing matrix Z_N is approximated as

$$Z_N \approx \begin{pmatrix} 1, & \frac{\lambda_a Y_\nu^* \upsilon}{\lambda_b^2 \upsilon_L}-, & \frac{\lambda_{b_1} Y_\nu^* \upsilon}{\lambda_b^2 \upsilon_L}, & \frac{\lambda_{b_2} Y_\nu^* \upsilon}{\lambda_b^2 \upsilon_L}, & \frac{\lambda_{b_3} Y_\nu^* \upsilon}{\lambda_b^2 \upsilon_L} \\ \frac{\lambda_a Y_\nu^* \upsilon}{\lambda_b^2 \upsilon_L}, & 0, & 0, & -\mathrm{i}\sqrt{\frac{\Delta+\lambda_a}{2\Delta}}, & \sqrt{\frac{\Delta-\lambda_a}{2\Delta}} \\ -\frac{\lambda_{b_1} Y_\nu^* \upsilon}{\lambda_b^2 \upsilon_L}, & -\frac{\lambda_{b_3}}{\sqrt{\lambda_{b_1}^2+\lambda_{b_3}^2}}, & -\frac{\lambda_{b_2}}{\sqrt{\lambda_{b_1}^2+\lambda_{b_2}^2}}, & \frac{\mathrm{i}\sqrt{2}\lambda_{b_1}}{\sqrt{\Delta^2+\lambda_a\Delta}}, & \frac{\sqrt{2}\lambda_{b_1}}{\sqrt{\Delta^2-\lambda_a\Delta}} \\ -\frac{\lambda_{b_2} Y_\nu^* \upsilon}{\lambda_b^2 \upsilon_L}, & 0, & 0, & \frac{\mathrm{i}\sqrt{2}\lambda_{b_2}}{\sqrt{\Delta^2+\lambda_a\Delta}}, & \frac{\sqrt{2}\lambda_{b_2}}{\sqrt{\Delta^2-\lambda_a\Delta}} \\ -\frac{\lambda_{b_3} Y_\nu^* \upsilon}{\lambda_b^2 \upsilon_L}, & \frac{\lambda_{b_1}}{\sqrt{\lambda_{b_1}^2+\lambda_{b_3}^2}}, & \frac{\lambda_{b_1}}{\sqrt{\lambda_{b_1}^2+\lambda_{b_2}^2}}, & \frac{\mathrm{i}\sqrt{2}\lambda_{b_3}}{\sqrt{\Delta^2+\lambda_a\Delta}}, & \frac{\sqrt{2}\lambda_{b_3}}{\sqrt{\Delta^2-\lambda_a\Delta}} \end{pmatrix}. \tag{33}$$

For the relevant parameters in the SM, we take [13]

$$\alpha_s(m_Z) = 0.118,\ \alpha(m_Z)=1/128,$$
$$s_W^2(m_Z) = 0.23,\ m_t=174.2 \text{ GeV},\ m_W=80.4 \text{ GeV}. \tag{34}$$

5.1 Numerical results of $R_{\gamma\gamma}$

Under our assumptions of the parameter space, the theoretical prediction of $R_{\gamma\gamma}$ depends on six parameters in the model: m_F, $m_{\phi^\pm}$, λ_{NP}, λ'_{NP}, υ_B and υ_L. Taking $m_{\phi^\pm}$=500 GeV, λ_{NP}=0.5 and $\lambda'_{NP}=-0.5$, we plot the variation of $R_{\gamma\gamma}$ with the mass scalar of exotic fermions M_F, as shown in Fig. 1. The dotted line corresponds to $\upsilon_B = \upsilon_L$=500 GeV, the dashed line corresponds to $\upsilon_B = \upsilon_L$=1000 GeV, and the solid line corresponds to $\upsilon_B = \upsilon_L$=1500 GeV. In general, the ratio $R_{\gamma\gamma}$ depends very weakly on the mass scale m_F, and the value of $R_{\gamma\gamma}$ is about 1.8–1.9 when 500 GeV$\leqslant \upsilon_B = \upsilon_L \leqslant$1500 GeV.

In Fig. 2(a), we plot the variation of $R_{\gamma\gamma}$ with the VEV υ_L when $m_{\phi^\pm} = \upsilon_B = 500$ GeV, $\lambda'_{NP}=-0.5$ and λ_{NP}=0.5. The dotted line corresponds to m_F=500 GeV, the dashed line corresponds to $m_F=550$ GeV, and the solid line corresponds to m_F=600 GeV. The dependence of $R_{\gamma\gamma}$ on υ_L is relatively sensitive for $\upsilon_L \leqslant$600 GeV, and is weak for $\upsilon_L>$600 GeV. Since the dependence of $R_{\gamma\gamma}$ on m_F and υ_B is very weak, the three lines almost coincide with each other. In Fig. 2(b), we plot the variation of $R_{\gamma\gamma}$ with the VEV υ_L when $m_F = m_{\phi^\pm} = \upsilon_B = 500$ GeV, $\lambda'_{NP}=-0.5$. The dotted line corresponds to $\lambda_{NP}=0.5$, the dashed line corresponds to λ_{NP}=0, and the solid line corresponds to $\lambda_{NP}=-0.5$. Generally, there is a weak dependence of the ratio $R_{\gamma\gamma}$ on υ_L.

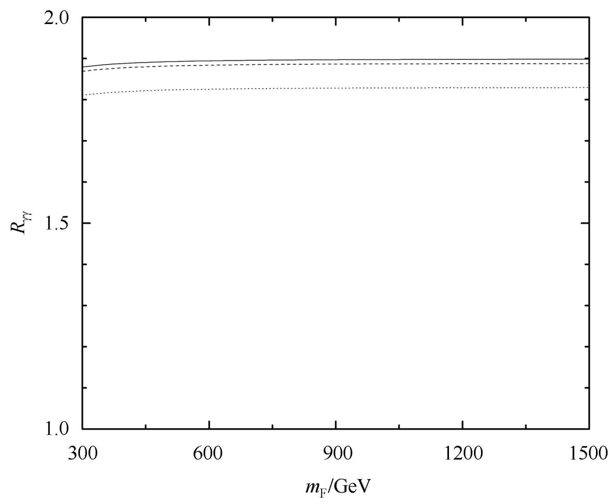

Fig. 1. Variation of $R_{\gamma\gamma}$ with the mass scale of exotic fermions m_F when $m_{\phi^\pm}$=500 GeV, λ_{NP}=0.5, $\lambda'_{NP}=-0.5$. The dotted line represents $\upsilon_B = \upsilon_L$=500 GeV, the dashed line represents $\upsilon_B = \upsilon_L$=1000 GeV, and the solid line represents $\upsilon_B = \upsilon_L$=1500 GeV.

In Fig. 3(a), we show the variation of $R_{\gamma\gamma}$ with the VEV υ_B when $m_F = \upsilon_L$=500 GeV, $\lambda_{NP}=0.5$. The dotted line corresponds to $\lambda'_{NP}=0.5$, the dashed line corresponds to $\lambda'_{NP}=0$, and the solid line corresponds to $\lambda'_{NP}=-0.5$. The dependence of $R_{\gamma\gamma}$ on υ_B is relatively sensitive for $\upsilon_B \leqslant$600 GeV, and is weak for $\upsilon_B>$600 GeV. In Fig. 3(b), we show the variation of $R_{\gamma\gamma}$ with υ_B when $m_F = \upsilon_L$=500 GeV, $\lambda'_{NP}=-0.5$ and λ_{NP}=0.5. The dotted line corresponds to $m_{\phi^\pm}$=1500 GeV, the dashed line

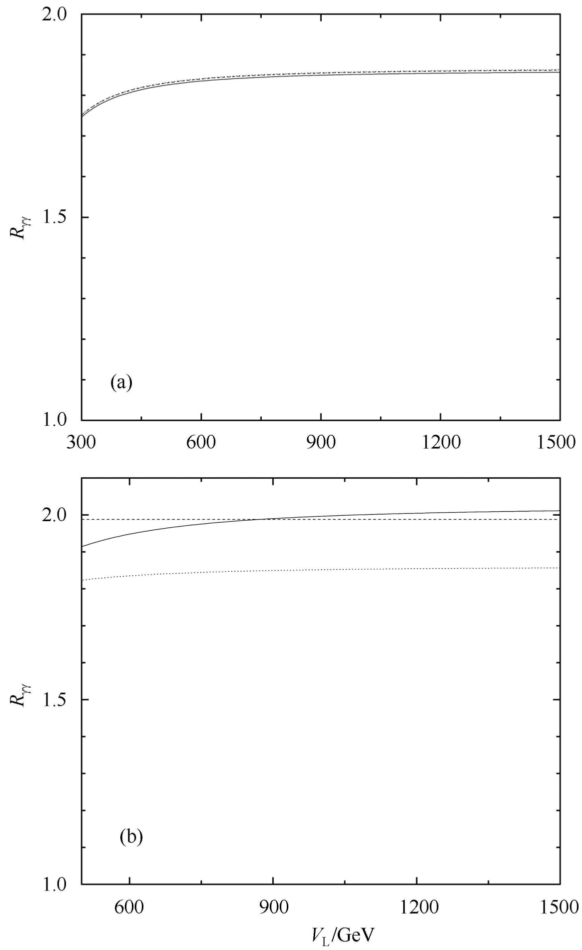

Fig. 2. Variation of $R_{\gamma\gamma}$ with the VEV υ_L when $m_{\phi^\pm}=\upsilon_B$=500 GeV, $\lambda'_{NP}=-0.5$. In (a), $\lambda_{NP}=0.5$, the dotted line corresponds to m_F=500 GeV, the dashed line corresponds to m_F=550 GeV, and the solid line corresponds to m_F=600 GeV. In (b), m_F=500 GeV, the dotted line corresponds to λ_{NP}=0.5, the dashed line corresponds to λ_{NP}=0, and the solid line corresponds to $\lambda_{NP}=-0.5$.

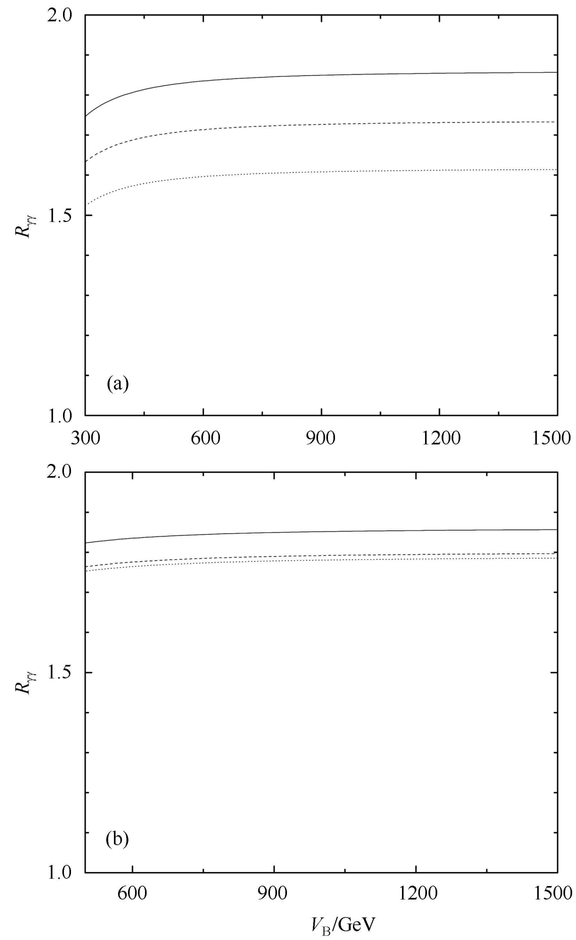

Fig. 3. Variation of $R_{\gamma\gamma}$ with the VEV υ_B when $m_F = \upsilon_L$=500 GeV, $\lambda_{NP} = 0.5$ for: (a) $m_{\phi^\pm}$=500 GeV, where the dotted line corresponds to λ'_{NP}=0.5, the dashed line corresponds to $\lambda'_{NP} = 0$, and the solid line corresponds to $\lambda'_{NP}=-0.5$; (b)$\lambda'_{NP}=-0.5$, where the dotted line corresponds to $m_{\phi^\pm}$=1500 GeV, the dashed line corresponds to $m_{\phi^\pm}$=1000 GeV, and the solid line corresponds to $m_{\phi^\pm}$=500 GeV.

corresponds to $m_{\phi^\pm}$=1000 GeV, and the solid line corresponds to $m_{\phi^\pm}$=500 GeV. Generally, there is a very weak dependence of the ratio $R_{\gamma\gamma}$ on υ_B.

Choosing $\upsilon_B = \upsilon_L$=500 GeV, $\lambda'_{NP} = -0.5$, Fig. 4 presents the variation of the ratio $R_{\gamma\gamma}$ with λ_{NP}. The dotted line represents m_F =500 GeV, $m_{\phi^\pm}$= 1500 GeV, the dashed line represents m_F =550 GeV, $m_{\phi^\pm}$ =1000 GeV, and the solid line represents $m_F = m_{\phi^\pm}$=500 GeV. As Λ_{NP} increases, $R_{\gamma\gamma}$ changes drastically and can easily coincide with the present experimental data, as $-0.5\leqslant\lambda_{NP}\leqslant 1.0$. Choosing $m_F=\upsilon_B=\upsilon_L$=500 GeV, and $\lambda_{NP} = -0.5$, Fig. 5 shows the ratio $R_{\gamma\gamma}$ versus $m_{\phi^\pm}$. The dotted line represents $\lambda'_{NP}=0.5$, the dashed line represents $\lambda'_{NP} = 0$, and the solid line represents $\lambda'_{NP} = -0.5$. For $\lambda'_{NP} = 0$, there is a slight dependence of $R_{\gamma\gamma}$ on the mass $m_{\phi^\pm}$. When $\lambda'_{NP}=\pm0.5$, $R_{\gamma\gamma}$ decreases steeply as $m_{\phi^\pm}$ increases.

In Fig. 6, we plot the variation of the ratio $R_{\gamma\gamma}$ with λ'_{NP} when $m_F=\upsilon_B=\upsilon_L$=500 GeV and $\lambda_{NP}=-0.5$. The dotted line represents $m_{\phi^\pm}$=1500 GeV, the dashed line represents $m_{\phi^\pm}$=1000 GeV, and the solid line represents $m_{\phi^\pm}$=500 GeV. The dependence of $R_{\gamma\gamma}$ on λ'_{NP} is strong when $m_{\phi^\pm}$=500 GeV but weaker for higher values of $m_{\phi^\pm}$.

Generally, the ratio $R_{\gamma\gamma}$ depends strongly on the parameters λ_{NP}, λ'_{NP} and $m_{\phi^\pm}$, and depends weakly on υ_B, υ_L and m_F. These numerical results can be reasonably explained from Eq. (18) and Eq. (19), where λ_{NP} affects theoretical predictions of $R_{\gamma\gamma}$ through the 3×3 mixing matrix Z_{CPE}, while λ'_{NP} and $m_{\phi^\pm}$ affect theoretical predictions of $R_{\gamma\gamma}$ through the last term in Eq. (19).

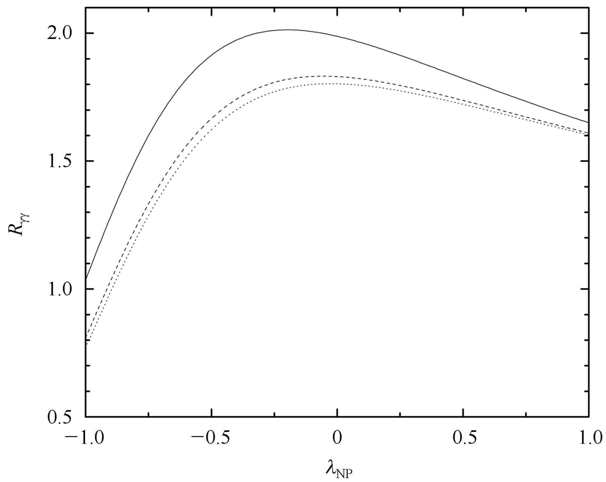

Fig. 4. Variation of $R_{\gamma\gamma}$ with λ_{NP} when $\upsilon_B = \upsilon_L$=500 GeV, $\lambda'_{NP} = -0.5$, where the dotted line represents m_F=500 GeV, $m_{\phi^\pm}$=1500 GeV, the dashed line represents m_F=550 GeV, $m_{\phi^\pm}$=1000 GeV, and the solid line represents m_F=$m_{\phi^\pm}$=500 GeV.

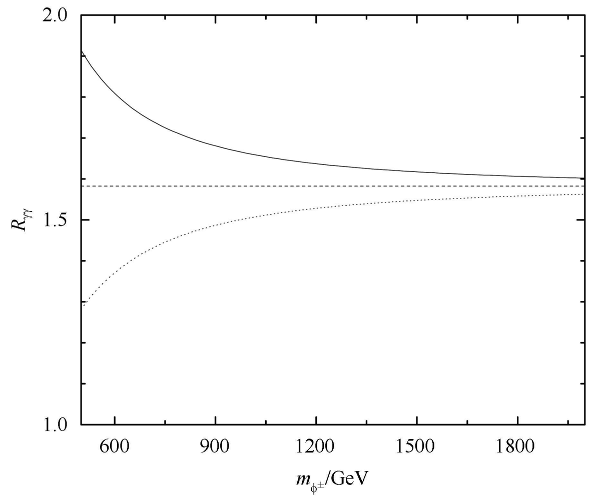

Fig. 5. Variation of $R_{\gamma\gamma}$ with $m_{\phi^\pm}$ when m_F=υ_B=υ_L=500 GeV, λ_{NP}=−0.5, where the dotted line represents $\lambda'_{NP}=0.5$, the dashed line represents λ'_{NP}=0, and the solid line represents λ'_{NP}=−0.5.

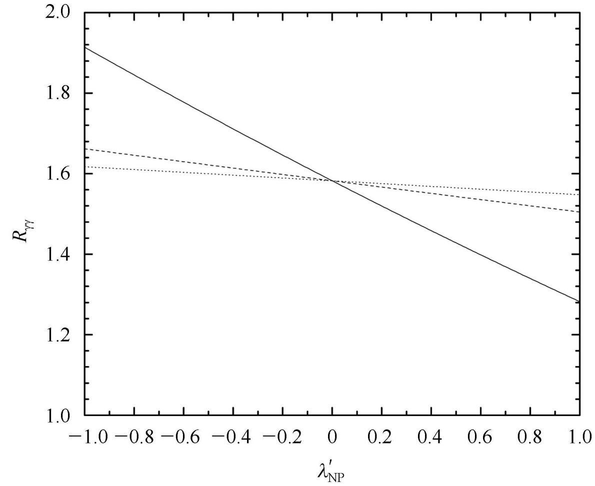

Fig. 6. Variation of $R_{\gamma\gamma}$ with λ'_{NP} when m_F=υ_B=υ_L=500 GeV, λ_{NP}=−0.5, where the dotted line represents $m_{\phi^\pm}$=1500 GeV, the dashed line represents $m_{\phi^\pm}$=1000 GeV, and the solid line represents $m_{\phi^\pm}$=500 GeV.

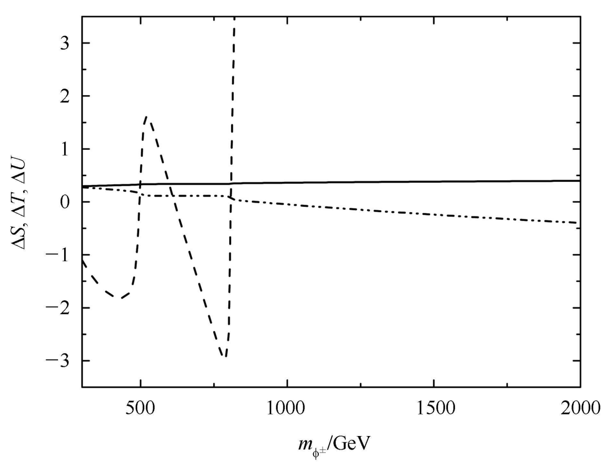

Fig. 7. Adopting the assumptions mentioned in the text and assuming θ_1=arg(μ_1)=π, θ_2=arg(μ_2)=π/4, we present the theoretical values for a) ΔS (solid line), b) ΔU (dash-dot-dot line), and c) ΔT (dashed line) versus the mass $m_{\phi^\pm}$.

The important point is that the parameters λ_a, λ_{b_i}(i=1, 2, 3) do not affect the theoretical predictions of $R_{\gamma\gamma}$ since there is no correction to the decay widths of $h_0\to\gamma\gamma$ and $h_0\to gg$ from the neutrino sector at one-loop level. Similarly, the parameters M_S, μ_1, μ_2 also do not affect theoretical evaluations of $R_{\gamma\gamma}$ because there is no one-loop correction to the decay widths of $h_0\to\gamma\gamma$ and $h_0\to gg$ from virtual Φ_i^0(i=1, 2, 3, 4).

5.2 The constraints on parameter space from oblique corrections

The heavy neutrinos contribute one-loop radiative corrections to the self energies of ZZ, $W^\pm W^\mp$ in this model. This results in the theoretical values of the S, T, U parameters depending on λ_a, λ_{b_i} (i=1, 2, 3) here. Furthermore, the theoretical values of the S, T, U parameters also depend on m_S, μ_1, μ_2 through the virtual $\phi^\pm$, Φ_i^0, (i=1, 2, 3, 4) radiative corrections to the self energies of ZZ, $W^\pm W^\mp$ at one-loop level. So far, fitting

S, T, U within 3σ deviation indicates

$$\begin{aligned}&-0.26\leqslant\Delta S\leqslant 0.34,\\&-0.28\leqslant\Delta T\leqslant 0.38,\\&-0.25\leqslant\Delta U\leqslant 0.41.\end{aligned}\qquad(35)$$

In order to obtain theoretical values of S, T, U that satisfy present experimental data, we adopt the following additional assumptions:

$$\begin{aligned}m_{\mathrm{N}_1}&\approx\frac{\upsilon^2}{\sqrt{2}\upsilon_{\mathrm{L}}}\frac{\lambda_{\mathrm{a}}|Y_\nu'|}{\lambda_{\mathrm{b}}^2}=m_{\mathrm{F}},\\ \lambda_{\mathrm{b}_1}&=\lambda_{b_2}=\lambda_{\mathrm{b}_3}=\frac{1}{\sqrt{3}}\lambda_{\mathrm{b}},\\ \upsilon_{\mathrm{B}}&=\upsilon_{\mathrm{L}}=m_{\mathrm{S}}=m_{\mathrm{F}}=500\ \mathrm{GeV},\\ |\mu_1|&=20\ \mathrm{GeV},\ |\mu_2|=200\ \mathrm{GeV},\\ \lambda_{\mathrm{a}}&=\lambda_{\mathrm{b}}=0.6,\ \lambda_{\mathrm{BB}}=\lambda_{\mathrm{LL}}=0.5,\ \lambda_{\mathrm{NP}}=\lambda_{\mathrm{NP}}'=0.01.\end{aligned}\qquad(36)$$

Choosing $\theta_1=\arg(\mu_1)=\pi$, $\theta_2=\arg(\mu_2)=\pi/4$, we depict the theoretical values of ΔS, ΔU, ΔT versus the mass of charged scalar $\phi^\pm$ in Fig. 7, in which the solid line represents ΔS, the dash-dot-dot line represents ΔU, and the dashed line represents ΔT. For our choices of the relevant parameters, the theoretical value of ΔT is very sensitive to the mass $m_{\phi^\pm}$, while the theoretical values of ΔS and ΔU have a weak dependence on the mass $m_{\phi^\pm}$. When the mass of the charged scalar lies in the range $400\leqslant m_{\phi^\pm}/\mathrm{GeV}\leqslant 700$, the theoretical predictions of ΔS, ΔT, ΔU simultaneously satisfy the inequalities in Eq. (35). The CP phases θ_1, θ_2 also affect the numerical results of ΔS, ΔU, ΔT through the 4×4 mixing matrix Z_{CPM}. Taking $m_{\phi^\pm}=600$ GeV and $\theta_2=\pi/4$, we present the theoretical evaluations on ΔS, ΔU, ΔT versus the CP phase θ_1 in Fig. 8. With our assumptions on the parameter space, the theoretical value of ΔT varies strongly with the CP phase θ_1, while the theoretical values of ΔS and ΔU vary weakly with the CP phase θ_1. In the neighbourhoods of $\theta_1=0$, $\pm\pi/2$, $\pm\pi$, the theoretical predictions on ΔS, ΔT, ΔU simultaneously lie within the ranges presented in Eq. (35).

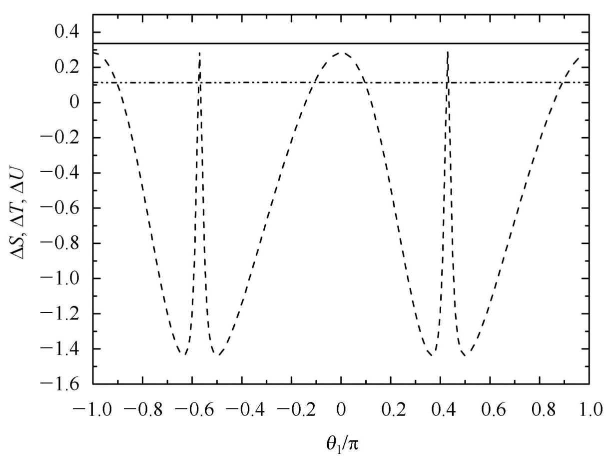

Fig. 8. Adopting the assumptions mentioned in the text and assuming $m_{\phi^\pm}=600$ GeV, $\theta_2=\arg(\mu_2)=\pi/4$, we present the theoretical values of a) ΔS (solid line), b) ΔU (dash-dot-dot line), and c) ΔT (dashed line) versus the CP phase $\theta_1=\arg(\mu_1)$.

In Fig. 9, we present the theoretical values of ΔS, ΔT, ΔU varying with the CP phase θ_2 when $m_{\phi^\pm}=600$ GeV and $\theta_1=\pi$. As the CP phase θ_2 varies, the theoretical value of ΔT changes drastically, while the theoretical values of ΔS and ΔU change slowly. In the neighbourhoods around $\theta_2=\pm\pi/4$, $\pm 3\pi/4$, the theoretical predictions of ΔS, ΔT, ΔU coincide with the present global EWPD fit within 3σ deviations.

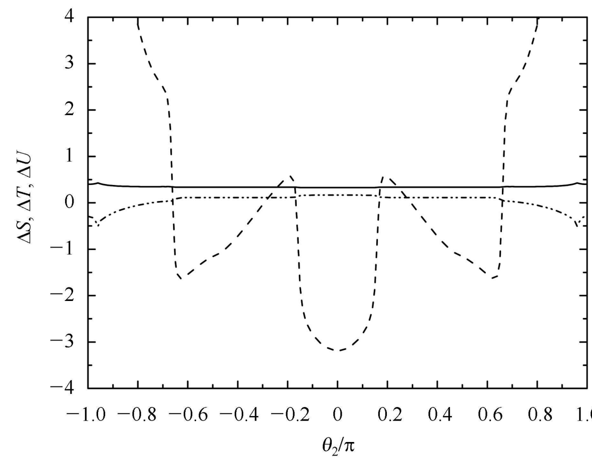

Fig. 9. Adopting the mentioned assumptions in text and assuming $m_{\phi^\pm}=600$ GeV, $\theta_1=\arg(\mu_1)=\pi$, we present the theoretical values of a) ΔS (solid line), b) ΔU (dash-dot-dot line), and c) ΔT (dashed line) versus the CP phase $\theta_2=\arg(\mu_2)$.

6 Summary

For an extension of the SM with local gauged baryon and lepton numbers, we have discussed the constraints from the oblique parameters S, T, U when the lightest Higgs has a mass around 125 GeV. Considering these constraints, we find that there is parameter space to account for the excess in Higgs production and decay in the diphoton channel observed in the ATLAS and CMS experiments. Of course, our numerical results strongly depend on the assumptions made in the model considered here. In other words, our theoretical prediction cannot be precise because of the theoretical uncertainties. The purpose of our calculation is to show that this extension of the SM may still be right even after the constraints from LHC data on the Higgs and oblique parameters have been taken into account.

Appendix A

Higgs masses and relevant couplings

After diagonalizing the mass matrix Eq. (5), we obtain

$$\begin{aligned} m_{\mathrm{h}_0}^2 &= \mathrm{Min}(m_1^2,\, m_2^2,\, m_3^2) \\ m_{\mathrm{H}_3^0}^2 &= \mathrm{Max}(m_1^2,\, m_2^2,\, m_3^2) \end{aligned} \tag{A1}$$

with

$$\begin{aligned} m_1^2 &= -\frac{a}{3}+\frac{2}{3}p\cos\phi, \\ m_2^2 &= -\frac{a}{3}-\frac{1}{3}p(\cos\phi-\sqrt{3}\sin\phi), \\ m_3^2 &= -\frac{a}{3}-\frac{1}{3}p(\cos\phi+\sqrt{3}\sin\phi). \end{aligned} \tag{A2}$$

To formulate the expressions in a concise form, we define the notations

$$p=\sqrt{a^2-3b},\phi=\frac{1}{3}\arccos\left(-\frac{1}{p^3}\left(a^3-\frac{9}{2}ab+\frac{27}{2}c\right)\right) \tag{A3}$$

where

$$\begin{aligned} a &= -2\Big(\lambda_{\mathrm{HH}}\upsilon^2+\lambda_{\mathrm{BB}}\upsilon_{\mathrm{B}}^2+\lambda_{\mathrm{LL}}\upsilon_{\mathrm{L}}^2\Big), \\ b &= 4(\lambda_{\mathrm{HH}}\lambda_{\mathrm{BB}}\upsilon^2\upsilon_{\mathrm{B}}^2+\lambda_{\mathrm{HH}}\lambda_{\mathrm{LL}}\upsilon^2\upsilon_{\mathrm{L}}^2+\lambda_{\mathrm{BB}}\lambda_{\mathrm{LL}}\upsilon_{\mathrm{B}}^2\upsilon_{\mathrm{L}}^2) \\ &\quad -\lambda_{\mathrm{HB}}^2\upsilon^2\upsilon_{\mathrm{B}}^2-\lambda_{\mathrm{HL}}^2\upsilon^2\upsilon_{\mathrm{L}}^2-\lambda_{\mathrm{BL}}^2\upsilon_{\mathrm{B}}^2\upsilon_{\mathrm{L}}^2, \\ c &= 2\Big(\lambda_{\mathrm{HH}}\lambda_{\mathrm{BL}}^2+\lambda_{\mathrm{BB}}\lambda_{\mathrm{HL}}^2+\lambda_{\mathrm{LL}}\lambda_{\mathrm{HB}}^2-4\lambda_{\mathrm{HH}}\lambda_{\mathrm{BB}}\lambda_{\mathrm{LL}} \\ &\quad -\lambda_{\mathrm{HB}}\lambda_{\mathrm{HL}}\lambda_{\mathrm{BL}}\Big)\upsilon^2\upsilon_{\mathrm{B}}^2\upsilon_{\mathrm{L}}^2. \end{aligned} \tag{A4}$$

The normalized eigenvectors of the mass squared matrix in Eq. (5) are given by

$$\begin{aligned} \begin{pmatrix} (Z_{\mathrm{CPE}})_{11} \\ (Z_{\mathrm{CPE}})_{21} \\ (Z_{\mathrm{CPE}})_{31} \end{pmatrix} &= \frac{1}{\sqrt{|X_1|^2+|Y_1|^2+|Z_1|^2}}\begin{pmatrix} X_1 \\ Y_1 \\ Z_1 \end{pmatrix}, \\ \begin{pmatrix} (Z_{\mathrm{CPE}})_{12} \\ (Z_{\mathrm{CPE}})_{22} \\ (Z_{\mathrm{CPE}})_{32} \end{pmatrix} &= \frac{1}{\sqrt{|X_2|^2+|Y_2|^2+|Z_2|^2}}\begin{pmatrix} X_2 \\ Y_2 \\ Z_2 \end{pmatrix}, \\ \begin{pmatrix} (Z_{\mathrm{CPE}})_{13} \\ (Z_{\mathrm{CPE}})_{23} \\ (Z_{\mathrm{CPE}})_{33} \end{pmatrix} &= \frac{1}{\sqrt{|X_3|^2+|Y_3|^2+|Z_3|^2}}\begin{pmatrix} X_3 \\ Y_3 \\ Z_3 \end{pmatrix}, \end{aligned} \tag{A5}$$

with

$$\begin{aligned} X_1 &= (2\lambda_{\mathrm{BB}}\upsilon_{\mathrm{B}}^2-m_1^2)(2\lambda_{\mathrm{LL}}\upsilon_{\mathrm{L}}^2-m_1^2)-\lambda_{\mathrm{BL}}^2\upsilon_{\mathrm{B}}^2\upsilon_{\mathrm{L}}^2, \\ Y_1 &= \lambda_{\mathrm{HL}}\lambda_{\mathrm{BL}}\upsilon\upsilon_{\mathrm{B}}\upsilon_{\mathrm{L}}^2-\lambda_{\mathrm{HB}}\upsilon\upsilon_{\mathrm{B}}(2\lambda_{\mathrm{LL}}\upsilon_{\mathrm{L}}^2-m_1^2), \\ Z_1 &= \lambda_{\mathrm{HB}}\lambda_{\mathrm{BL}}\upsilon\upsilon_{\mathrm{B}}^2\upsilon_{\mathrm{L}}-\lambda_{\mathrm{HL}}\upsilon\upsilon_{\mathrm{L}}(2\lambda_{\mathrm{BB}}\upsilon_{\mathrm{B}}^2-m_1^2), \\ X_2 &= \lambda_{\mathrm{HL}}\lambda_{\mathrm{BL}}\upsilon\upsilon_{\mathrm{B}}\upsilon_{\mathrm{L}}^2-\lambda_{\mathrm{HB}}\upsilon\upsilon_{\mathrm{B}}(2\lambda_{\mathrm{LL}}\upsilon_{\mathrm{L}}^2-m_2^2), \\ Y_2 &= (2\lambda_{\mathrm{HH}}\upsilon^2-m_2^2)(2\lambda_{\mathrm{LL}}\upsilon_{\mathrm{L}}^2-m_2^2)-\lambda_{\mathrm{HL}}^2\upsilon^2\upsilon_{\mathrm{L}}^2, \\ Z_2 &= \lambda_{\mathrm{HB}}\lambda_{\mathrm{HL}}\upsilon^2\upsilon_{\mathrm{B}}\upsilon_{\mathrm{L}}-\lambda_{\mathrm{BL}}\upsilon_{\mathrm{B}}\upsilon_{\mathrm{L}}(2\lambda_{\mathrm{HH}}\upsilon^2-m_2^2), \\ X_3 &= \lambda_{\mathrm{HB}}\lambda_{\mathrm{BL}}\upsilon\upsilon_{\mathrm{B}}^2\upsilon_{\mathrm{L}}-\lambda_{\mathrm{HL}}\upsilon\upsilon_{\mathrm{L}}(2\lambda_{\mathrm{BB}}\upsilon_{\mathrm{B}}^2-m_3^2), \\ Y_3 &= \lambda_{\mathrm{HB}}\lambda_{\mathrm{HL}}\upsilon^2\upsilon_{\mathrm{B}}\upsilon_{\mathrm{L}}-\lambda_{\mathrm{BL}}\upsilon_{\mathrm{B}}\upsilon_{\mathrm{L}}(2\lambda_{\mathrm{HH}}\upsilon^2-m_3^2), \\ Z_3 &= (2\lambda_{\mathrm{HH}}\upsilon^2-m_3^2)(2\lambda_{\mathrm{BB}}\upsilon_{\mathrm{B}}^2-m_3^2)-\lambda_{\mathrm{HB}}^2\upsilon^2\upsilon_{\mathrm{B}}^2. \end{aligned} \tag{A6}$$

Appendix B

The loop functions

The loop functions in Eq. (18) and Eq. (19) are given as

$$\begin{aligned} A_1(x) &= -\Big[2x^2+3x+3(2x-1)g(x)\Big]/x^2, \\ A_{1/2}(x) &= 2\Big[x+(x-1)g(x)\Big]/x^2, \\ A_0(x) &= -(x-g(x))/x^2, \end{aligned} \tag{B1}$$

with

$$g(x)=\begin{cases} \arcsin^2\sqrt{x}, x\leqslant 1 \\ -\dfrac{1}{4}\left[\ln\dfrac{1+\sqrt{1-1/x}}{1-\sqrt{1-1/x}}-\mathrm{i}\pi\right]^2, \ x>1 \end{cases} \tag{B2}$$

References

1 Peskin M E, Takeuchi T. Phys. Rev. Lett., 1999, **65**: 964; Phys. Rev. D, 1992, **46**: 381; Marciano W J, Rosner J L. Phys. Rev. Lett., 1999, **65**: 2963

2 Holdom B, Terning J. Phys. Lett. B, 1990, **247**: 88; Golden M, Randall L. Nucl. Phys. B, 1991, **361**: 3; Altarelli G, Barbieri R. Phys. Lett. B, 1990, **253**: 161; Altarelli G, Barbieri R, Jadach S. Nucl. Phys. B, 1992, **369**: 3

3 Minkoski P. Phys. Lett. B, 1977, **67**: 421; Yanagida T. Proceedings of the Workshop on the Unified Theory and the Baryon Number in the Universe, KEK, Tsukuba, 1979. 95; Gell-Mann M, Ramond P, Slansky R. Supergravity. North-Holland, Amsterdam, 1979. 315; Glashow S L. Quarks and Leptons, Cargése. New York: Plenum, 1980. 707; Mohapatra R N, Senjanovic G. Phys. Rev. Lett., 1980, **44**: 912

4 Perez P F, Wise M B. Phys. Rev. D, 2010, **82**: 011901; 2011, **84**: 055015; Dulaney T R, Perez P F, Wise M B. Phys. Rev. D, 2011, **83**: 023520; CHANG C H, FENG T F. Eur. Phys. J. C, 2000, **12**: 137

5 Perez P F. Phys. Lett. B, 2012, **711**: 353; Arnold J M, Perez P F, Fornal B, Spinner S. Phys. Rev. D, 2012, **85**: 115024

6 Anastasiou C, Melnikov K. Nucl. Phys. B, 2002, **646**: 220

7 Ellis J R, Gaillard M K, Nanopoulos D V. Nucl. Phys. B, 1976, **106**: 292; Shifman M A, Vainshtein A I, Voloshin M B, Zakharov V I. Sov. J. Nucl. Phys., 1979, **30**: 711; Djouadi A. Phys. Rept., 2008, **459**: 1; Gunion J F, Haber H E, Kane G L, Dawson S. The Higgs Hunter's Guide, Addison-Wesley, Reading (USA), 1990; Carena M, Low I, Wagner C E M. arXiv: hep-ph/ 1206.1082

8 CMS collaboration, CMS-PAS-HIG-12-016

9 ATLAS collaboration, ATLAS-CONF-2012-092

10 Arbey A, Battaglia M, Djouadi A, Mahmoudi F. arXiv: hep-ph/ 1207.1348

11 HE H J, Polonsky N, SU S F. Phys. Rev. D, 2001, **64**: 053004

12 Baak M, Goebel M, Haller J, Hoecker A, Ludwig D, Moenig K, Schott M, Stelzer J. Eur. Phys. J. C, 2012, **72**: 2003

13 Beringer J et al. (Particle Data Group). Phys. Rev. D, 2012, **86**: 010001